Coagulation equations with mass loss

JONATHAN A.D. WATTIS, D. GRAHAM MCCARTNEY[1] and THROSTUR GUDMUNDSSON[2]
Theoretical Mechanics, School of Mathematical Sciences, University of Nottingham, University Park, Nottingham, NG7 2RD, UK; [1]*School of Mechanical, Materials, Manufacturing Engineering and Management, University of Nottingham, University Park, Nottingham, NG7 2RD, UK;* [2]*VST Engineers, Armula 4, 108 Reykjavik, Iceland; (e-mails: Jonathan.Wattis@nottingham.ac.uk; Graham.McCartney@nottingham.ac.uk)*

Abstract. Models for coagulation with mass loss arising, for example, from industrial processes in which growing inclusions are lost from the melt by colliding with the wall of the vessel are derived and solved. A variety of loss laws and a variety of coagulation kernels are considered, exact results derived where possible, and more generally the equations are reduced and solved by similarity solutions valid in the large-time limit. One notable result is the effect that mass removal has on gelation: for small loss rates, gelation is delayed, whilst above a critical threshold, gelation is completely prevented. Finally, by forming an exact explicit solution for a more general initial cluster-size distribution function, it is shown how numerical results from earlier work can be interpreted in the light of the theory presented herein.

Key words: aggregation, cluster-size distribution, Smoluchowski coagulation

1. Introduction

Aluminium and its alloys are of increasing importance in many industrial sectors for packaging, transport and construction uses. In recent years, there has been a growing recognition that in many applications material performance is limited by the presence of micrometre-sized, insoluble inclusions that are introduced into the molten metal by melting and refining processes which are conducted prior to the casting of ingots or components; for examples see [1] and [2]. Critical properties of, for example, ultra-thin foil and thin strip for the packaging industry can be adversely affected by the presence of such non-metallic inclusions.

In the production of aluminium alloys, molten metal is held in a furnace for periods of up to several hours before it is cast. At this stage, sub-micrometre-sized particles of the insoluble, high-melting-point chemical compound titanium diboride (TiB_2) are added for the purpose of efficiently nucleating solid aluminium during subsequent solidification and casting [3]. However, whilst the melt is held in the furnace, these TiB_2 particles can both agglomerate and also be lost from the melt by attachment to the furnace walls. Both processes are extremely undesirable, and practical steps taken to minimise agglomeration and loss, or to remove coarse agglomerates, lead to significantly increased manufacturing costs. Although there have been considerable advances in the capability to measure inclusion content and size distribution in molten aluminium, for example see [4], there is still a lack of understanding of the kinetics of coagulation in this system. It is in this context that the present study was undertaken.

Over recent years, generalised forms of Smoluchowski's coagulation equations have been developed to model the size-evolution of clusters of particles in such systems. Leyvraz and

Tschudi [5] have noted that the coagulation equations without mass loss could be solved exactly if the coagulation rates were given by one of two special kernels, that is a function which specifies how the rate of coagulation depends on the size of the aggregating clusters. The solvable cases which they describe are the size-independent kernel $a_{i,j} = a$ and the size-dependent kernel $a_{i,j} = a(i + j)$. Our approach originally outlined in [6] uses generating functions, and delivers explicit solutions more simply. This method has been extended to model situations with mass addition [7] and mass loss through direct interaction between clusters and the gel [8].

Singh and Rodgers [9] considered aggregation processes which occur simultaneously with mass loss in the framework of a continuous model. They consider the scenario where oxidation, melting or evaporation occur on the exposed surface of clusters, and hence take the mass-loss term to have the form $-\frac{\partial}{\partial j}(m(j)c(j,t))$, where $c(j,t)$ or $c_j(t)$ denotes the concentration of clusters of size j at time t. Hendriks [10] also considers aggregation with mass loss, but only when the aggregation kernel has the form $a_{i,j} = aij$; this is the classic kernel which allows gelation and an exact explicit solution in the case of pure coagulation. The mass-loss term used by Hendriks has a similar form to that used by us, namely, $\mathcal{L}_j = Ac_j + Bjc_j$ in the notation introduced later on. Finally, we should note the work of Rotstein *et al.* [11] in which a mass-loss term is introduced in the monomer equation. In a similar way to the more general loss term we consider, their term can delay or totally prevent gelation in the case of the coagulation kernel which permits gelation to occur; they analyse how the amount of gel formed depends on the strength of the rate of mass removal.

1.1. MODEL

We use C_k to denote a cluster composed of k monomers. The kinetics of the standard Smoluchowski agglomeration process

$$C_i + C_j \rightarrow C_{i+j}, \quad \text{rate} = a_{i,j} \tag{1.1}$$

with aggregation rate $a_{i,j}$ can be modelled by defining the concentration of C_j to be $c_j(t)$. Using the law of mass action we then obtain

$$\frac{dc_j(t)}{dt} = \frac{1}{2}\sum_{i=1}^{j-1} a_{i,j-i}c_i(t)c_{j-i}(t) - \sum_{i=1}^{\infty} a_{i,j}c_i(t)c_j(t). \tag{1.2}$$

Deriving the second sum is more straightforward than the first; it comes from the fact that a cluster C_j can combine with a cluster C_i of any size $1 \leq i < \infty$ as described by (1.1). Thus we sum over all i to obtain the rate at which C_j clusters are lost due to aggregation. The first sum in (1.2) comes from the rate at which C_j clusters are created by the coalescence of smaller clusters through $C_i + C_{j-i} \rightarrow C_j$. The factor of one half is present to prevent double counting of this process. Since matter is neither created nor destroyed in the coagulation process, we expect the total number of monomers in the system $M_1 = \sum_{j=1}^{\infty} jc_j$ to be time-independent. As a check of (1.2), M_1 can be shown formally to be a constant. More details about this calculation are given at the start of Section 2.3. To the standard Smoluchowski coagulation equations (1.2) we add a mass-loss term of the form $C_j \rightarrow \phi$ with rate $\mathcal{L}_j(c_j)$; hence we obtain the system of equations

$$\frac{dc_j(t)}{dt} = \frac{1}{2}\sum_{i=1}^{j-1} a_{i,j-i}c_i(t)c_{j-i}(t) - \sum_{i=1}^{\infty} a_{i,j}c_i(t)c_j(t) - \mathcal{L}_j(c_j(t)). \tag{1.3}$$

In the model of interest to Gudmundsson [12] the clusters are micrometre-sized non-metallic inclusions (TiB_2) in molten aluminium and the aggregation rates are determined by $a_{i,j} = (R_i + R_j)(D_i + D_j)$. Here R_i is the radius of a sphere with volume iV_0 for some element of volume V_0, thus $R_i \propto i^{1/3}$; D_i is the corresponding diffusion constant, with $D_i \propto 1/R_i$. This corresponds to the continuum regime of Brownian coagulation. Many other kernels have been used to model aggregation processes, see [13] for examples. In the process analysed by Gudmundsson, mass is lost by removal of particles from the melt by transfer to the walls of the holding furnace for the molten metal. This occurs at a rate $\mathcal{L}_j(c_j(t)) = Lj^\lambda c_j(t)$ for some L and $\lambda = 2/3$.

We shall consider a more general problem, in which λ is not constrained to $2/3$, but could take any value, and in which the coagulation kernel has the form $a_{i,j} = ai^\alpha j^\alpha(i^\beta + j^\beta)$. This covers the integrable cases $a_{i,j} = a$ ($\alpha = \beta = 0$), as well as $a_{i,j} = a(i + j)$ ($\alpha = 0$, $\beta = 1$), and $a_{i,j} = aij$ ($\alpha = 1$, $\beta = 0$). The Brownian kernel of Gudmundsson corresponds to a combination of the constant kernel $a_{i,j} = a$ and the case $\alpha = -1/3$, $\beta = 2/3$.

We thus have the system of equations

$$\frac{dc_j(t)}{dt} = \tfrac{1}{2}\sum_{i=1}^{j-1} a_{i,j-i}c_i(t)c_{j-i}(t) - \sum_{i=1}^{\infty} a_{i,j}c_i(t)c_j(t) - Lj^\lambda c_j(t), \qquad (1.4)$$

which models the simultaneous aggregation and mass-loss processes. It is the presence of a mass-loss term which is novel in the current study of the coagulation equations. We describe cases in which information about the solution can be derived exactly and explicitly; this corresponds to the case $\lambda = 0$, where the generating-function approach yields a complete solution. The existence of a closed-form exact solution to such a complicated system of equations is remarkable, and the solution for $\lambda > 0$ will share many properties of the solution for $\lambda = 0$. We then examine the case of general λ in more detail, by use of large-time asymptotic methods, and by assuming the existence of a self-similar solution, which enables various scaling behaviours of the solution to be elucidated. In the analysis of gelation in a truncated version of Smoluchowski's coagulation equations, da Costa derived an equation of the form (1.4), namely Equation (10) of [13]; however, there $L < 0$ corresponding to a mass gain term, and the second sum has an upper limit of $i = N$ in place of $i = \infty$. Similarity solutions of the form derived below should still be applicable in this case; however, the derivations of exact explicit solutions for the three integrable coagulation kernels will be complicated by the finite sum.

The paper is split into five sections. In the next section we derive exact explicit solutions for models where these are available. Section 3 describes the similarity solutions which the system may approach in the large-time limit. A more general approach to the fitting of exact solutions to experimental data and numerical simulations is described in Section 4. The paper concludes with a summary and discussion of the results.

2. Explicitly solvable models

2.1. SIZE-INDEPENDENT AGGREGATION RATES

The special case of the parameters being given by $a_{i,j} = a$, $\lambda = 0$ is exactly solvable, this corresponds to the system

$$\frac{dc_j}{dt} = \frac{1}{2}\sum_{i=1}^{j-1} ac_ic_{j-i} - \sum_{i=1}^{\infty} ac_ic_j - Lc_j. \tag{2.1}$$

We introduce the generating function $C(z, t) = \sum_{j=1}^{\infty} c_j(t)e^{-jz}$, which transforms the system of ordinary differential equations (2.1) to

$$\frac{\partial C}{\partial t} = \frac{1}{2}aC^2 - C(L + aM_0(t)), \tag{2.2}$$

where $M_0(t) = C(0, t)$ is the total number of clusters in the system. This quantity satisfies

$$\frac{dM_0}{dt} = -\frac{1}{2}M_0(aM_0 + 2L), \tag{2.3}$$

and so is given by

$$M_0(t) = \frac{2L\varrho e^{-Lt}}{2L + a\varrho(1 - e^{-Lt})}, \tag{2.4}$$

where we have assumed monodisperse initial conditions

$$c_j(0) = 0, \qquad \text{for } j > 1 \quad c_1(0) = \varrho. \tag{2.5}$$

These conditions imply $C(z, 0) = \varrho e^{-z}$; hence we solve (2.2) to find

$$C(z, t) = \frac{4\varrho L^2 e^{-Lt}}{(2L + a\varrho(1 - e^{-Lt}))^2}\left(\frac{2L + a\varrho(1 - e^{-Lt})}{2Le^z + a\varrho(1 - e^{-Lt})(e^z - 1)}\right) \tag{2.6}$$

for the generating function $C(z, t)$ and the concentrations $c_j(t)$ are then given by

$$c_j(t) = \frac{4\varrho L^2 e^{-Lt}}{(2L + a\varrho(1 - e^{-Lt}))^2}\left(\frac{a\varrho(1 - e^{-Lt})}{2L + a\varrho(1 - e^{-Lt})}\right)^{j-1}. \tag{2.7}$$

This solution is illustrated in Figure 1. We see that, at small times, aggregation is dominant, which rapidly creates an appreciable number of clusters of larger size. At larger times, there is a slower decrease in the concentration of clusters of all sizes. For large cluster sizes ($j \gg 1$), the maximum concentration occurs at

$$t_c(j) \sim \frac{1}{L}\log\left(\frac{(2L + a\varrho)j}{2L}\right). \tag{2.8}$$

For larger times the solution (2.7), can be approximated by

$$c_j(t) \sim \frac{4L^2 e^{-Lt}}{a(2L + a\varrho)}\left(\frac{a\varrho}{2L + a\varrho}\right)^j, \tag{2.9}$$
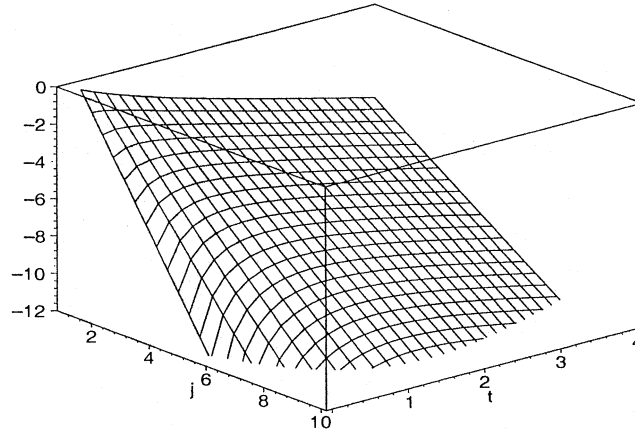
Figure 1. Figure of the exact solution (2.7), $\log c_j(t)$ is plotted against size j and time t, for $1 \leq j \leq 10$ and $0 < t < 4$ for the case $\varrho = 1$, $L = 1$, $a = 1$.

which corresponds to the late-time depletion of all clusters by loss predominantly due to the explicit mass-removal term, that is, loss to the walls of the container.

From such a solution other quantities of interest may be found, for example, the first few moments are given by Equation (2.4) and

$$M_1(t) = \varrho\, e^{-Lt}, \qquad M_2(t) = \varrho e^{-Lt}\left(1 + \frac{a\varrho}{L}(1 - e^{-Lt})\right), \tag{2.10}$$

since

$$M_1(t) = -\frac{\partial C}{\partial z}(0, t), \qquad M_2(t) = \frac{\partial^2 C}{\partial z^2}(0, t). \tag{2.11}$$

This agrees with the experimental results of Gudmundsson [12] where he observes a decay in the total volume of the material which is exponential. The average cluster size is given by either M_1/M_0, or M_2/M_1; these give similar expressions

$$\frac{M_1}{M_0} = 1 + \frac{a\varrho}{2L}(1 - e^{-Lt}), \qquad \frac{M_2}{M_1} = 1 + \frac{a\varrho}{L}(1 - e^{-Lt}). \tag{2.12}$$

Initially, both give unity, since all material starts in clusters of unit size; as time progresses, the former rises steadily to $1 + a\varrho/2L$, while the latter approaches $1 + a\varrho/L$. A measure of the spread of the distribution can be gained from the polydispersity

$$\frac{M_2 M_0}{M_1^2} = 1 + \frac{a\varrho(1 - e^{-Lt})}{2L + a\varrho(1 - e^{-Lt})}. \tag{2.13}$$

This quantity is initially equal to one, indicating a monodisperse system and rises to $1 + a\varrho/(a\varrho + 2L)$ in the large-time limit.

2.2. SIZE-DEPENDENT AGGREGATION RATES

In the case $a_{i,j} = a(i + j)$ the coagulation equations have the form

$$\frac{dc_j}{dt} = \tfrac{1}{2}a \sum_{i=1}^{j-1} jc_i c_{j-i} - ac_j \sum_{i=1}^{\infty}(i + j)c_i - Lc_j. \tag{2.14}$$

We use the same generating function as earlier ($C(z, t) = \sum_{j=1}^{\infty} c_j(t)e^{-jz}$), to rewrite the above as

$$\frac{\partial C}{\partial t} = a\frac{\partial C}{\partial z}(M_0 - C) - aM_1C - LC, \tag{2.15}$$

subject to the initial data (2.5), which imply $C(z, 0) = \varrho e^{-z}$. The mass and number in the system are then governed by

$$\frac{dM_1}{dt} = -LM_1, \qquad \frac{dM_0}{dt} = -M_0(aM_1 + L), \tag{2.16}$$

which are solved by

$$M_1(t) = \varrho e^{-Lt}, \qquad M_0(t) = \varrho \exp\left(-Lt - \frac{a\varrho}{L}(1 - e^{-Lt})\right). \tag{2.17}$$

As with the size-independent kernel, this confirms the exponential decay of the total mass in the system; however, this solution is based on $\lambda = 0$ and not $\lambda = 2/3$, as was assumed by Gudmundsson. The above solutions for M_0 and M_1 allow solving (2.15) by the method of characteristics, which gives the implicit solution

$$-z = \log\frac{C}{\varrho} + Lt + \frac{a\varrho}{L}(1 - e^{-Lt}) + \tag{2.18}$$
$$\left[1 - \exp\left(-\frac{a\varrho}{L}(1 - e^{-Lt})\right)\right]\left[1 - \frac{Ce^{Lt}}{\varrho}\exp\left(\frac{a\varrho}{L}(1 - e^{-Lt})\right)\right].$$

This is inverted by use of Lagrange's expansion (see [14, Equation 3.6.6]), which yields

$$\begin{aligned}
c_j(t) &= \frac{\varrho j^{j-1}}{j!}e^{-Lt-T}(1 - e^{-T})^{j-1}e^{-j(1-e^{-T})} \\
&= \frac{\varrho e^{-Lt}j^{j-1}}{j!}\widehat{T}^{j-1}e^{-j\widehat{T}}(1 - \widehat{T}),
\end{aligned} \tag{2.19}$$

where $T = (\varrho a/L)(1 - e^{-Lt})$ and $\widehat{T} = 1 - e^{-T}$. This solution is illustrated in Figure 2.

The second moment can also be determined, from $dM_2/dt = 2aM_1M_2 - LM_2$, we find

$$M_2(t) = \varrho e^{-Lt}\exp\left(\frac{2a\varrho}{L}(1 - e^{-Lt})\right). \tag{2.20}$$

There are then two ways of defining the typical size of a cluster in the system, which give very similar expressions

$$\frac{M_2}{M_1} = \exp\left(\frac{2a\varrho}{L}(1 - e^{-Lt})\right), \qquad \frac{M_1}{M_0} = \exp\left(\frac{a\varrho}{L}(1 - e^{-Lt})\right), \tag{2.21}$$

and the polydispersity of the system (which is related to the variance of the cluster size distribution) is given by

$$\frac{M_2M_0}{M_1^2} = \exp\left(\frac{a\varrho}{L}(1 - e^{-Lt})\right). \tag{2.22}$$
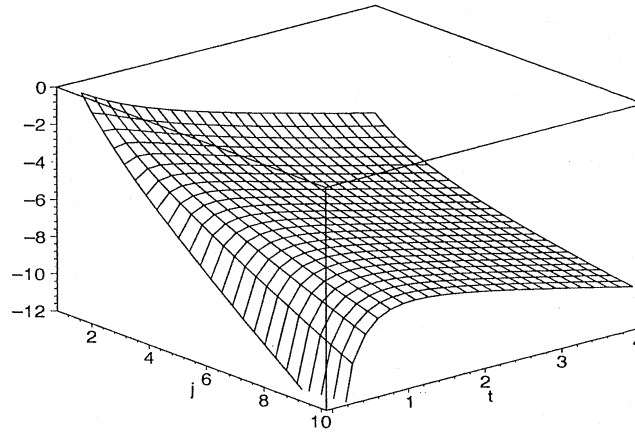
Figure 2. Figure of the exact solution (2.19), $\log c_j(t)$ is plotted against size j and time t, for $1 \leq j \leq 10$ and $0 < t < 4$ for the case $\varrho = 1$, $L = 1$, $a = 1$.

All these formulae assume that the initial conditions are monodisperse, that is, given by (2.5).

2.3. THE GELLING KERNEL

A natural question to ask is whether the presence of the explicit mass-loss term alters gelation. In the absence of a mass-loss term (that is, if $L = 0$), the system (1.2) satisfies

$$\frac{\mathrm{d}jc_j}{\mathrm{d}t} = J_{j-1} - J_j, \qquad \text{where} \quad J_j = \sum_{k=1}^{j} \sum_{n=j+1-k}^{\infty} ka_{n,k}c_nc_k. \tag{2.23}$$

Formally, we have $\mathrm{d}M_1/\mathrm{d}t = -\lim_{N\to\infty} J_N$. If this limit is zero, mass is conserved and, if it is non-zero, the system loses mass to a cluster of infinite size, known as the 'superparticle' or the 'gel'. Intuitively we expect that, for large enough λ (or L), the shape of the cluster-size distribution will be altered at large sizes, and so gelation could be prevented; however, for small (possibly negative) λ or small L, the mass-loss term may have no effect on gelation. In the case $\lambda = 0$ the system is once again exactly explicitly solvable as we now show. The generating function in this case reduces the differential-difference equation

$$\frac{\mathrm{d}c_j}{\mathrm{d}t} = \tfrac{1}{2} \sum_{i=1}^{j-1} ai(j-i)c_ic_{j-i} - ajc_j \sum_{i=1}^{\infty} ic_i - Lc_j \tag{2.24}$$

to

$$\frac{\partial C}{\partial t} = \tfrac{1}{2}a \left(\frac{\partial C}{\partial z} \right)^2 + aM_1 \frac{\partial C}{\partial z} - LC, \tag{2.25}$$

with initial data $C(z,0) = \varrho e^{-z}$. Defining $u = -\partial C/\partial z$ we find the partial differential equation

$$\frac{\partial u}{\partial t} + a(u - M_1(t))\frac{\partial u}{\partial z} = -Lu. \tag{2.26}$$

2.3.1.   *Pre-gel behaviour*

Equations governing the number and mass of clusters can be found by putting $z = 0$ into (2.25) and (2.26). This leads to

$$\frac{\mathrm{d}M_1}{\mathrm{d}t} = -LM_1, \qquad \frac{\mathrm{d}M_0}{\mathrm{d}t} = -\tfrac{1}{2}M_1^2 - LM_0, \tag{2.27}$$

which have the solutions

$$M_1(t) = \varrho \mathrm{e}^{-Lt}, \quad M_0(t) = \varrho \mathrm{e}^{-Lt}\left(1 - \frac{a\varrho}{2L}(1 - \mathrm{e}^{-Lt})\right). \tag{2.28}$$

These formulae are only valid in the pre-gelation stage of the process. The partial differential equation (2.26) is solved by the method of characteristics, leading to

$$z = \log \varrho - \log u - Lt + \frac{au}{L}(\mathrm{e}^{Lt} - 1) - a\int_0^t M_1(s)\,\mathrm{d}s. \tag{2.29}$$

In the pregel phase, M_1 is given by (2.28) and so we find

$$\mathrm{e}^{-z} = \frac{u\mathrm{e}^{Lt}}{\varrho}\exp\left(-\frac{a\mathrm{e}^{Lt}}{L}(1 - \mathrm{e}^{-Lt})(u - \varrho\mathrm{e}^{-Lt})\right), \tag{2.30}$$

which can be inverted using Lagrange's expansion, yielding

$$c_j(t) = \frac{\varrho j^{j-2}\mathrm{e}^{-Lt}}{j!}\left(\frac{\varrho a(1 - \mathrm{e}^{-Lt})}{L}\right)^{j-1}\exp\left(\frac{-\varrho aj(1 - \mathrm{e}^{-Lt})}{L}\right), \tag{2.31}$$

or $c_j(t) = \varrho \mathrm{e}^{-Lt}j^{j-2}T^{j-1}\mathrm{e}^{-jT}/j!$ where $T = \varrho a(1 - \mathrm{e}^{-Lt})/L$. Note that this new time variable satisfies $T \to a\varrho/L$ as $t \to \infty$. In the limit $L \to 0$ with $\varrho = a = 1$, this reduces to the classical solution pre-gelation solution, $c_j(t) = j^{j-2}t^{j-1}\mathrm{e}^{-jt}/j!$, where gelation occurs at $t = t_g = 1$. Thus in the general solution for $L \neq 0$, gelation occurs at $T_g = 1$. So if $L > \varrho a$ then gelation is prevented by the mass-loss term since $T = 1$ is never reached, even in the limit $t \to \infty$, whereas for $L < \varrho a$ gelation is merely delayed from $t_g = 1/\varrho a$ to

$$t_g = -\frac{1}{L}\log\left(1 - \frac{L}{a\varrho}\right). \tag{2.32}$$

For small L this asymptotes to $t_g \sim (1/\varrho a)(1 + L/2\varrho a)$; and $t_g \to \infty$ as $L \to \varrho a$.

For general initial data, information on the gelation behaviour of the system can be gained from the second moment. Here we shall not assume that the initial conditions are monodisperse, rather we assume that $M_1(0) = \varrho$ and $M_2(0) = \mu$. The second moment is determined by $\mathrm{d}M_2/\mathrm{d}t = aM_2^2 - LM_2$ which shows that, for sufficiently large L, the possibility of gelation may be removed. The solution for $M_2(t)$ is

$$M_2(t) = \frac{\mu L}{a\mu + [L - a\mu]\mathrm{e}^{Lt}}. \tag{2.33}$$

In the pre-gel regime the typical cluster size is given by

$$\frac{M_1}{M_0} = \frac{2L}{2L - a\varrho(1 - \mathrm{e}^{-Lt})}, \qquad \frac{M_2}{M_1} = \frac{L\mu}{L\varrho - a\varrho\mu(1 - \mathrm{e}^{-Lt})}, \tag{2.34}$$

and the polydispersity by

$$\frac{M_2 M_0}{M_1^2} = \frac{2L\mu - a\varrho\mu(1 - e^{-Lt})}{2L\varrho - 2a\varrho\mu(1 - e^{-Lt})}. \tag{2.35}$$

The gel-point occurs at the time at which the second moment diverges (that is $M_2 \to \infty$ as $t \to t_g$), which implies

$$t_g = -\frac{1}{L} \log\left(1 - \frac{L}{a\mu}\right). \tag{2.36}$$

Thus gelation only occurs if $\mu > L/a$. There is an interesting issue about the sensitive dependence of gelation to initial data: for example, one can perturb the monodisperse initial data (2.5) by adding in a small concentration (of order $\varepsilon \ll 1$) of one particular very large cluster size (size $j \sim 1/\sqrt{\varepsilon}$). This makes an $\mathcal{O}(\varepsilon)$ difference to the total number of clusters at time $t = 0$, an $\mathcal{O}(\sqrt{\varepsilon})$ difference to the mass of the system at $t = 0$, but at $\mathcal{O}(1)$ difference to the second moment of the system. Thus this perturbation can make the difference between a solution undergoing gelation and not. Thus, when analysing cluster size-distributions, it is important to use a measure or norm which takes account of the second moment.

2.3.2. *Post-gel behaviour*

As the gel-point is approached ($t \to t_g$), a singularity develops, namely $u_z \to -\infty$ at $z = 0$; this corresponds to the divergence in the second moment, $M_2(t)$. The post-gel solution is characterised by persistence of the singularity in u_z at $z = 0$. By differentiating (2.29) with respect to z we find

$$\frac{\partial u}{\partial z} = \frac{Lu}{au(e^{Lt} - 1) - L}, \tag{2.37}$$

and so, substituting $z = 0$ in this, we find

$$M_1(t) = u(0, t) = \frac{L}{a(e^{Lt} - 1)} \quad \text{for } t > t_g. \tag{2.38}$$

It can be checked that at $t = t_g$ the formula (2.38) gives $M_1 = \varrho - L/a$ as does (2.28); thus M_1 is continuous across the gel-point $t = t_g$.

We now return to (2.29) with $M_1(t)$ given by (2.28) for $t < t_g$ and by (2.38) for $t > t_g$. In this latter region we then find

$$e^{-z} = \frac{eau}{L}(e^{Lt} - 1)e^{-au(e^{Lt}-1)/L}, \tag{2.39}$$

and applying Lagrange's expansion once again, we obtain

$$c_j(t) = \frac{L j^{j-2} e^{-j}}{a j! (e^{Lt} - 1)}. \tag{2.40}$$

Thus, as $j \to \infty$, we have the usual post-gel algebraic decay in cluster size with $c_j \sim L/\sqrt{2\pi} a j^{5/2}(e^{Lt} - 1)$. Note that: (i) this formula and (2.40) are independent of the initial mass in the system, ϱ; (ii) (2.40) is a similarity solution of separable form, $c_j(t) = f_j/\tau(t)$; and, (iii) from (2.40) we determine the number of clusters in the post-gel regime. At $t = t_g$
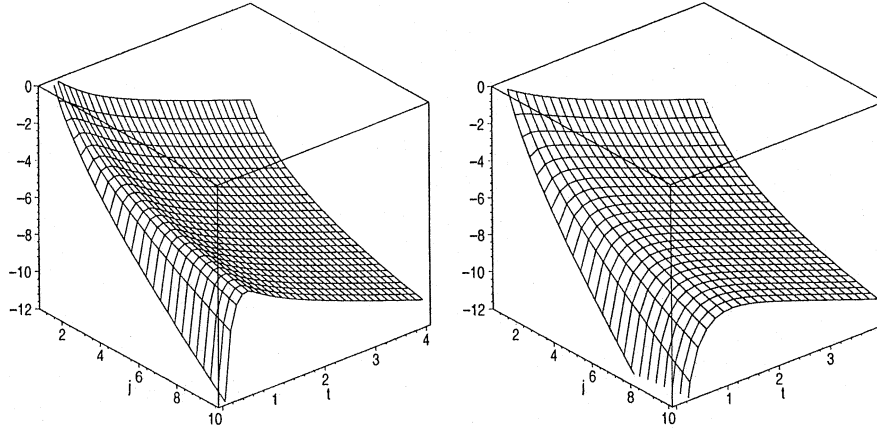
Figure 3. The exact solution (2.31) for $t < t_g$ and (2.40) for $t > t_g$; $\log c_j(t)$ is plotted against size j and time t for $1 \leq j \leq 10$ and $0 < t < 4$; on the left for $\varrho = 2$, $L = 1$, $a = 1$, so that the gel-time $t_g = \log 2$; on the right for $\varrho = 1$, $L = 1$, $a = 1$, so that there is no gelation ($t_g = \infty$).

Equation (2.28) implies $M_0(t_g) = \varrho(1 - L/a\varrho)/2$, which can then be used as initial data for the ordinary differential equation for $M_0(t)$ in (2.27) to yield the post-gel solution

$$M_0(t) = \frac{L}{2a(e^{Lt} - 1)}, \qquad t \geq t_g. \tag{2.41}$$

A gelling solution is illustrated in Figure 3, where the gel-time is $\log 2$.

A natural question to consider in this scenario is how much of the initial mass ends up in the gelled form and how much is removed by the explicit mass-loss term, and so ends up adhered to the wall. To analyse this, we introduce two new quantities: $W(t)$ is the mass adhered to the wall, and $G(t)$ the mass in the gel. Thus we have $M_1(t) + G(t) + W(t) = \varrho$ independent of time. In the pre-gel phase, $G = 0$, $W = \varrho - M_1$; and, as $t \to \infty$, $M_1 \to 0$, so in the large time limit we have $G + W = \varrho$. We also have $dW/dt = \sum_{j=1}^{\infty} Lj^{\lambda+1}c_j$, which, in the case of $\lambda = 0$, simplifies to $dW/dt = LM_1$. In the pre-gel phase of the reaction, integrating $dW/dt = LM_1$ yields

$$W(t) = (\varrho/L)(1 - e^{-Lt}), \qquad (t \leq t_g); \tag{2.42}$$

thus, at the gel-point we have $W(t_g) = L/a$ (assuming monodisperse initial data (2.5)). Integrating $dW/dt = LM_1$ in the post-gel phase, where $M_1(t)$ is given by (2.38), yields

$$W(t) = \frac{L}{a}\left(1 + \log(1 - e^{-Lt}) - \log\left(\frac{L}{a\varrho}\right)\right), \qquad (t \geq t_g). \tag{2.43}$$

Thus, ultimately the mass deposited on the wall and in the gelled form is given by

$$W_\infty = \frac{L}{a}\left(1 - \log\left(\frac{L}{a\varrho}\right)\right), \qquad G_\infty = \varrho - W_\infty, \tag{2.44}$$

provided $L < a\varrho$. If $L \geq a\varrho$, the mass-loss term prevents gelation, and so all mass eventually ends up on the wall. Thus, if we look at the proportion of mass adhering to the wall ($\Phi = W_\infty/\varrho$) as a function of the nondimensional parameter group $L/a\varrho$, we have the function

$$\Phi(L/a\varrho) = \begin{cases} (1 - \log(L/a\varrho))L/a\varrho, & L/a\varrho < 1, \\ 1, & L/a\varrho \geq 1, \end{cases} \tag{2.45}$$
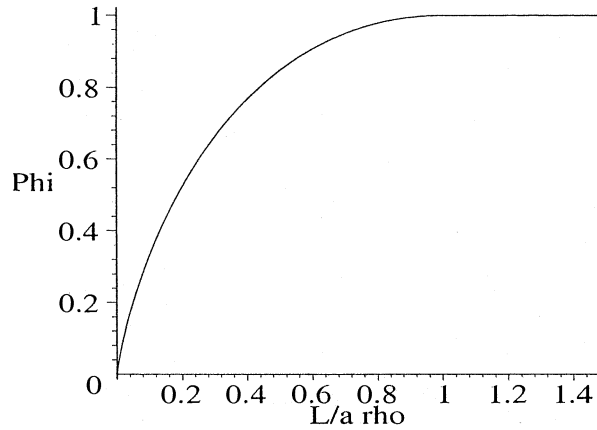
Figure 4. Graph of proportion of mass ultimately adhered to the wall against the dimensionless parameter $L/a\varrho$ which indicates the rate of loss of matter from the system.

which is continuous and has a continuous first derivative, but has a discontinuous second derivative. To illustrate this, we consider values of $L/a\varrho$ close to unity, we put $L/a\varrho = 1 - \varepsilon$ with $0 < \varepsilon \ll 1$ and then find that $\Phi \sim 1 - \frac{1}{2}\epsilon^2$. Thus Φ rises from zero at $L = 0$ to its upper limit at $L/a\varrho = 1$ where we obtain $\Phi = 1$ as shown in Figure 4.

3. Similarity solutions

The existence of similarity solutions to the Smoluchowski coagulation equations has been the subject of much study, analytically, by Kreer and Penrose [15] and da Costa [16] and by asymptotic methods, for example, by Hendriks *et al.* [17], and more recently by Davies *et al.* [6]. Gudmundsson [12] speculated on the existence of similarity solutions to the mass-losing coagulation equations. Here we show that such solutions may exist in the case $\lambda < 0$.

3.1. SIZE-INDEPENDENT AGGREGATION RATES

For $a_{i,j} = a$, we seek a solution of the form $c_j(t) = t^\gamma f(\eta)$ where $\eta = jt^\beta$ is the similarity variable. We substitute the *ansatz* in Equation (1.4), and find that all terms balance, provided $\beta = 1/\lambda$, $\gamma = 1/\lambda - 1$. Since β should be negative, we require λ also to be negative for a similarity solution of this form to exist. Such a scaling satisfies the density conservation equation $dM_1/dt = -LM_{\lambda+1}$ since $M_1 \sim \mathcal{O}(t^{\gamma-2\beta})$, and $M_{\lambda+1} \sim \mathcal{O}(t^{\gamma-(\lambda+2)\beta})$. From such calculations we find

$$M_0(t) = \Phi_0 t^{-1}, \quad M_1(t) = \Phi_1 t^{-1-1/\lambda}, \quad M_2(t) = \Phi_2 t^{-1-2/\lambda}, \tag{3.1}$$

where $\Phi_k = \int_{\eta=0}^\infty \eta^k f(\eta)\, d\eta$, and so if M_1 is to be well-defined we require $\lambda < -1$. The average cluster size, which is given by M_1/M_0 or M_2/M_1, increases according to $t^{-1/\lambda}$. The polydispersity $M_2 M_0/M_1^2$ is constant (independent of time) once the similarity solution has been approached. With $\lambda < 0$, smaller clusters are removed at a faster rate than larger ones, so that the total number of clusters decays faster than the mass in the system, and higher moments diverge more rapidly, leading to a cluster-size distribution in which higher moments, cease to exist.

The function $f(\eta)$ satisfies

$$\frac{(1-\lambda)}{\lambda} f + \frac{\eta}{\lambda} \frac{\mathrm{d}f}{\mathrm{d}\eta} = \tfrac{1}{2} a \int_0^\eta f(\xi) f(\eta - \xi) \, \mathrm{d}\xi - a\Phi_0 f - L\eta^\lambda f, \tag{3.2}$$

where $\Phi_0 = \int_0^\infty f(\xi) \, \mathrm{d}\xi$. Unfortunately, in general, such equations are not solvable; however, for large and small η, asymptotic approximations for $f(\eta)$ are available.

For small η the leading-order balance is between the rate of change term, $\eta f'(\eta)/\lambda$, and the mass-loss term, $L\eta^\lambda f(\eta)$. This gives the expression $f(\eta) \sim \mathrm{e}^{-L\eta^\lambda}$. A correction term can be calculated by substituting $f(\eta) = \mathrm{e}^{-L\eta^\lambda} g(\eta)$ in (3.2). This leads to

$$\left(\frac{1}{\lambda} - 1 \right) g + \frac{\eta}{\lambda} \frac{\mathrm{d}g}{\mathrm{d}\eta} + a\Phi_0 g = 0 \tag{3.3}$$

at the next order of accuracy, the convolution being much smaller than these terms. This expression is solved by $g(\eta) = A\eta^q$ for some amplitude A and exponent q given by $q = \lambda - 1 - \lambda a \Phi_0$. Thus we have the expression

$$f(\eta) \sim A\eta^{\lambda-1-\lambda a \Phi_0} \mathrm{e}^{-L\eta^\lambda}, \quad \text{for } \eta \ll 1, \tag{3.4}$$

and

$$c_j(t) \sim A j^{\lambda-1-\lambda a \Phi_0} t^{-a\Phi_0} \mathrm{e}^{-Lj^\lambda t}, \tag{3.5}$$

as $t \to \infty$ and for $j \ll t^{-1/\lambda}$.

For large η, the leading-order balance is between the creation of new clusters as described by the convolution term, the loss by coagulation and the rate of change terms, from which we have

$$\frac{\eta}{\lambda} \frac{\mathrm{d}f}{\mathrm{d}\eta} + \left(\frac{1}{\lambda} - 1 + a\Phi_0 \right) f = a \int_0^{\eta/2} f(\xi) f(\eta - \xi) \, \mathrm{d}\xi. \tag{3.6}$$

If we assume $f(\xi)$ is given by the small-argument asymptotic expansion (3.4) and all the other occurrences of f are given by the large-η asymptotic expansion $f(\eta) \sim B\eta^q$ for some B, q then we find that all the terms on the left-hand side of (3.6) balance with the contribution to the integral from the small-ξ range, and that this places no restrictions on the values of B or q. Considering now the part of the integral where $\xi \sim \eta$, we find that, to balance all terms, we require $q = -1$ and then

$$a\Phi_0 = \tfrac{1}{2} a B \int_0^1 \frac{\mathrm{d}x}{x(1-x)}, \tag{3.7}$$

where the divergences at the end-points of the integral can be ignored, since an alternative expression for f should be used there, namely (3.4). Thus, for large η we have

$$f(\eta) \sim B/\eta, \quad \text{as } \eta \to +\infty, \tag{3.8}$$

and therefore $c_j \sim B/jt$ as $t \to \infty$ with $j \gg t^{-1/\lambda}$.

For the coagulation kernel suggested by Gudmundsson, namely $a_{i,j} = 2 + (i/j)^\omega + (j/i)^\omega$ with $\omega = 1/3$, the scalings for a similarity solution are exactly the same as for the constant

kernel $a_{i,j} = a$. The equation for the self-similar function $f(\eta)$ is, however, different, and so has different large- and small-η asymptotics:

$$\frac{\eta}{\lambda}\frac{\mathrm{d}f}{\mathrm{d}\eta} + \left(\frac{1}{\lambda} - 1\right) f + L\eta^{\lambda} f + a\left(2\Phi_0 + \eta^{\omega}\Phi_{-\omega} + \eta^{-\omega}\Phi_{\omega}\right) f$$
$$= \tfrac{1}{2}a \int_0^{\eta} f(\xi)f(\eta - \xi)\left[2 + \left(\frac{\eta - \xi}{\xi}\right)^{\omega} + \left(\frac{\xi}{\eta - \xi}\right)^{\omega}\right]\,\mathrm{d}\xi. \tag{3.9}$$

Hence

$$f(\eta) \sim A\eta^q \exp\left(-L\eta^{\lambda} + \frac{\lambda a \Phi_{\omega}}{\omega \eta^{\omega}}\right) \quad \text{as} \ \ \eta \to 0^+ \tag{3.10}$$

for some exponent q and some amplitude A; whilst

$$f(\eta) \sim B\eta^{\omega - 1} \quad \text{for} \ \ \eta \gg 1, \tag{3.11}$$

for some constant B.

3.2. SIZE-DEPENDENT AGGREGATION RATES

For $a_{i,j} = a(i + j)$ the coagulation equations have the form

$$\frac{\mathrm{d}c_j}{\mathrm{d}t} = \tfrac{1}{2}a \sum_{i=1}^{j-1} jc_i c_{j-i} - ac_j \sum_{i=1}^{\infty}(i + j)c_i - Lj^{\lambda}c_j. \tag{3.12}$$

Assuming $c_j(t) = t^{\gamma} f(j/t^{\beta})$ we find $\gamma = 2/\lambda - 1$, $\beta = -1/\lambda$, and $f(\eta)$ is determined by

$$\left(\frac{2}{\lambda} - 1\right) f \ + \ \frac{\eta}{\lambda}\frac{\mathrm{d}f}{\mathrm{d}\eta} + L\eta^{\lambda} f(\eta) + a\Phi_1 f(\eta) + a\Phi_0 \eta f(\eta)$$
$$= \tfrac{1}{2}a\eta \int_0^{\eta} f(\xi)f(\eta - \xi)\,\mathrm{d}\xi. \tag{3.13}$$

The regime $\eta = \mathcal{O}(1)$ corresponds to $j = \mathcal{O}(t^{-1/\lambda})$, and in general cannot be solved.

In the large-time limit, for $\lambda > 0$, it is the small-η limit which is of interest, since this corresponds to aggregation sizes $j \ll t^{-1/\lambda}$. As only a little mass gets into the large cluster sizes before being removed from the system, knowledge of the behaviour of such smaller cluster sizes is more important in physical applications. Thus, we consider in more detail the small-η asymptotic solution of (3.13). At leading order the balance is between $\eta f'/\lambda$ and $L\eta^{\lambda} f$, which produces the solution $f = \mathrm{e}^{-L\eta^{\lambda}}$ as in the case of the size-independent coagulation kernel. The first correction term, however, differs; we substitute $f = \mathrm{e}^{-L\eta^{\lambda}} g(\eta)$ to determine the prefactor of the exponent, and obtain the equation

$$\left(\frac{2}{\lambda} - 1 + a\Phi_1\right) g + \frac{\eta}{\lambda}\frac{\mathrm{d}g}{\mathrm{d}\eta} = 0, \tag{3.14}$$

This implies $g(\eta) \sim \eta^{\lambda - 2 - \lambda a \Phi_1}$, and we thus have

$$f(\eta) \sim A\eta^{\lambda - 2 - \lambda a \Phi_1}\mathrm{e}^{-L\eta^{\lambda}} \quad \text{for} \ \ \eta \ll 1. \tag{3.15}$$

The asymptotic solution for $c_j(t)$ is then

$$c_j(t) = Aj^{\lambda-2-a\lambda\Phi_1}t^{-a\Phi_1}e^{-Lj^\lambda t} \quad \text{as } t \to \infty \text{ with } j \ll t^{-1/\lambda}. \tag{3.16}$$

For completeness, we quote the large-η asymptotics; due to the nonlocal nature of (3.13), isolating the large-η asymptotics is not straightforward. At large η, the dominant terms govern the formation of clusters by the integral term, and the loss by collision with other clusters, thus from (3.13) we aim to solve

$$a\Phi_0\eta f = \tfrac{1}{2}a\eta \int_0^\eta f(\xi)f(\eta-\xi)\,\mathrm{d}\xi, \tag{3.17}$$

for which $f(\eta) = B\eta^q$ appears to be a solution for $q = -1$ and $B = 2\Phi_0/\int_0^1(x(1-x))^{-1}\,\mathrm{d}x$. However, this integral is divergent. The solution $f(\eta) = B\eta^{-1}$ remains, since the divergence is caused by integrating the function $f(\xi)$ near $\xi = 0$, where f is not given by $B\xi^{-1}$ but by (3.15) instead. With this modification, the solution $f(\eta) = B\eta^{-1}$ remains valid for large η, but the expression for B cannot be evaluated without knowing $f(\eta)$ across the whole range of values from $\eta = 0$ up to large η. Large η corresponds to $j \ll t^{-1/\lambda}$ and so we have

$$c_j(t) \sim \frac{B}{jt^{1-1/\lambda}} \quad \text{as } t \to \infty \quad \text{with } j \ll t^{-1/\lambda}. \tag{3.18}$$

3.3. GELLING KERNEL

For $a_{i,j} = aij$ we have seen that there is a gelation point if $\lambda = 0$ and $L < aM_2(0)$, and in this case, the post-gel solution corresponds to a similarity solution; from (2.40) we see that the appropriate scalings are $c_j(t) = f_j/(e^{Lt} - 1)$. When $\lambda < 0$ the loss is predominantly taken from smaller cluster sizes, with larger cluster sizes having smaller loss rates. Since gelation occurs due to the very slow decay of concentrations with increasing cluster size, loss rates with negative λ will not prevent the formation of a distribution function with a slowly decaying tail. Thus, with small L, and large $M_2(0)$ gelation should still occur, and we expect the post-gel solution to have the form of a similarity solution.

Assuming $c_j(t) = t^\gamma f(jt^\beta)$, we find a similarity solution, provided $\beta = 1/\lambda$ and $\gamma = 3/\lambda - 1$. The form of $f(\eta)$ is then given by

$$\frac{\eta}{\lambda}\frac{\mathrm{d}f}{\mathrm{d}\eta} + L\eta^\lambda f(\eta) + (3\lambda - 1)f(\eta) + a\Phi_1\eta f(\eta)$$

$$= \tfrac{1}{2}a\int_0^\eta \xi f(\xi)(\eta-\xi)f(\eta-\xi)\,\mathrm{d}\xi. \tag{3.19}$$

A solution of this equation is not available explicitly; however, some properties of the solution can be deduced by considering the small- and large-η behaviour of a solution. Also, the behaviour of certain quantities can be derived, for example

$$M_0(t) \sim t^{2/\lambda-1}\int_0^\infty f(\eta)\,\mathrm{d}\eta, \quad M_1(t) \sim t^{1/\lambda-1}\int_0^\infty \eta f(\eta)\,\mathrm{d}\eta. \tag{3.20}$$

For small η, the leading-order balance is between the rate-of-change term $\eta f'(\eta)/\lambda$ and the loss term $L\eta^\lambda f(\eta)$, leading to $f(\eta) = g(\eta)e^{-L\eta^\lambda}$ as in previous cases. The correction term is then determined by solving

$$\left(\frac{3}{\lambda} - 1\right)g + \frac{\eta}{\lambda}\frac{\mathrm{d}g}{\mathrm{d}\eta} = 0, \tag{3.21}$$

the convolution term being smaller than these retained terms. From the above equation we find $g(\eta) = A\eta^{\lambda-3}$ and we have

$$c_j(t) \sim A j^{\lambda-3} e^{-Lj^\lambda t} \quad \text{as } t \to \infty \quad \text{for } j \ll t^{-1/\lambda}, \tag{3.22}$$

for some constant A.

For large η, the leading-order balance is

$$a\Phi_1 \eta f = \tfrac{1}{2} a \int_0^\eta \xi f(\xi)(\eta - \xi) f(\eta - \xi) \, \mathrm{d}\xi, \tag{3.23}$$

that is, between for the formation of clusters of scaled size η by coagulation and the loss by coagulation. This leads to the asymptotic expression $f(\eta) \sim B/\eta^2$ for some constant B. Thus, we have

$$c_j(t) \sim \frac{B}{j^2 t^{1-1/\lambda}} \quad \text{as } t \to \infty \quad \text{with } j \gg t^{-1/\lambda}. \tag{3.24}$$

3.4. More general coagulation kernels

We consider some more general coagulation kernels, and show that the above analysis remains applicable. For the general coagulation kernel $a_{i,j} = a(ij)^\alpha (i^\beta + j^\beta)$ we find the similarity variable is $\eta = jt^{1/\lambda}$ again, with the concentrations $c_j(t)$ being given by $t^{-1+(1+2\alpha+\beta)/\lambda} f(\eta)$. The function $f(\eta)$ is then given by

$$\frac{\eta}{\lambda} \frac{\mathrm{d}f}{\mathrm{d}\eta} - \left(1 - \frac{1+2\alpha+\beta}{\lambda}\right) f + L\eta^\lambda f + a(\Phi_{\alpha+\beta} + \eta^\beta \Phi_\alpha)\eta^\alpha f$$
$$= \tfrac{1}{2} a \int_{\xi=0}^\eta \xi^\alpha f(\xi)(\eta - \xi)^\alpha f(\eta - \xi)(\xi^\beta + (\eta - \xi)^\beta) \, \mathrm{d}\xi. \tag{3.25}$$

Assuming $\alpha, \beta > 0$ we find the following asymptotic results hold: for $\eta \ll 1$, $f(\eta) \sim \eta^{\lambda-1-2\alpha-\beta} e^{-L\eta^\lambda}$, thus

$$c_j(t) \sim A j^{\lambda-1-2\alpha-\beta} e^{-Lj^\lambda t}, \quad \text{as } t \to \infty \quad \text{with } j \ll t^{-1/\lambda}; \tag{3.26}$$

and $f(\eta) \sim B\eta^{-1-\alpha}$ when $\eta \gg 1$, thus

$$c_j(t) \sim B j^{1/\lambda} t^{-1+(\alpha+\beta)/\lambda} \quad \text{as } t \to \infty \quad \text{with } j \gg t^{-1/\lambda}. \tag{3.27}$$

In the case of diffusion-controlled growth of supported metal crystallite, the aggregation kernel is $a_{i,j} = i^{-\beta} + j^{-\beta}$, with $\beta = 2/3$. In this case, following an analysis similar to that presented above, we obtain the similarity solution $c_j \sim t^{(1-\lambda-\beta)/\lambda} f(\eta)$ with $\eta = jt^{1/\lambda}$. For small η the asymptotic solution is $f(\eta) \sim A\eta^q \exp(-L\eta^\lambda + \lambda a\Phi_0 \eta^{-\beta}/\beta)$ with $q = \beta + \lambda - 1 - \lambda a\Phi_{-\beta}$, implying

$$c_j(t) \sim A j^q t^{1/\lambda - a\Phi_{-\beta}} \exp\left(-Lj^\lambda t + \frac{\lambda a\Phi_0}{\beta j^\beta t^{\beta/\lambda}}\right) \quad \text{as } t \to \infty \quad \text{with } j \ll t^{-1/\lambda}. \tag{3.28}$$

However, in the application we are concerned with here, which is a stirred chamber, the case of aggregation in a linear shear-velocity profile is perhaps more relevant. This corresponds to
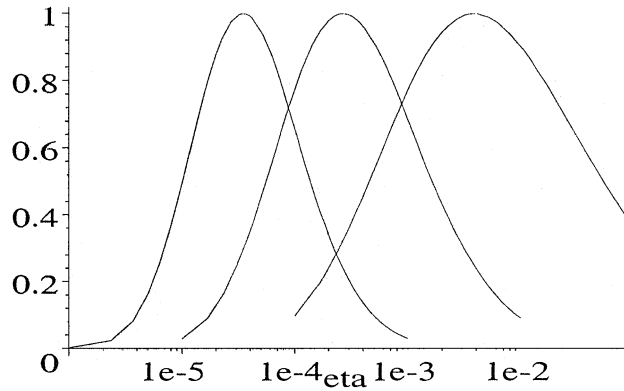
Figure 5. Graph of the similarity function $f(\eta)/f(\eta_c)$ against $\log \eta$ for small η; for the kernels $a_{i,j} = 1$ (on the right), $a_{i,j} = i + j$ (in the centre), $a_{i,j} = ij$ (on the left).

$a_{i,j} = (i^{1/3} + j^{1/3})^3$, and so, following an analysis similar to the above, we find the similarity solution $c_j(t) = t^{-1+2/\lambda} f(jt^{1/\lambda})$, where the distribution $f(\eta)$ is given by $f(\eta) \sim A\eta^p e^{-L\eta^\lambda}$ as $t \to \infty$ for $j \ll t^{-1/\lambda}$; here the constants A, p must satisfy $p = \lambda - 2 - \lambda a \Phi_1$ where $\lambda < 0$ and $\Phi_1 = \int_0^\infty \xi f(\xi) \, d\xi$.

3.5. SMALL-η RESULTS

For each of the kernels considered above, the small-η asymptotics have the form $f(\eta) = A\eta^q e^{-L\eta^\lambda}$ with $q < 0$. This has the form of a single-humped function, with maximum at $\eta_c = (q/\lambda L)^{1/\lambda}$. Thus, provided this occurs at $\eta_c \ll 1$, the form of the similarity solution will also be single-humped, the maximum having amplitude $f(\eta_c) = Aqe^{-q/\lambda}/\lambda L$. The form of such functions is illustrated in Figure 5, where results are shown for the case $L = 1$, $a = 1$, $\Phi_0 = 1$, $\Phi_1 = 1\cdot2$, $\lambda = -0\cdot25$.

4. Match to experimental results

The exact solutions given in Section 2 did not have the form observed in the numerical simulations of Gudmundsson (see [12] and [18]). One reason for this may be the differences in the kernel used; in numerical work, Gudmundsson used the more accurate kernel $a_{i,j} = 2 + (i/j)^{1/3} + (j/i)^{1/3}$ for Brownian coagulation, whereas the theory of Section 2 considered the simpler kernels $a_{i,j} = a$, $a_{i,j} = a(i + j)$. Another reason is that in Section 2 we only considered $\lambda = 0$, whereas Gudmundsson took $\lambda = 2/3$ in his numerical simulations. Finally, for algebraic simplicity we used monodisperse initial data (2.5), whereas more-complex initial data were considered by Gudmundsson. We would have to resort to numerical techniques to solve most of the more accurate cases; however, more-complicated initial data can be handled by the generating-function method of Section 2 and a solution still obtained. In this section we specify a more general form of initial data, for example, a single-humped size distribution as given by

$$c_j(0) = Aje^{-j\xi}, \tag{4.1}$$

for some ξ. The maximum of this distribution occurs at $j = 1/\xi$. Using such initial data, we can still apply the exact method of solution outlined in Section 2, although the algebra is more complicated.

The initial data for the system are

$$C(z, 0) = \frac{A\,e^{z+\xi}}{(e^{z+\xi} - 1)^2}, \qquad\qquad M_0(0) = \frac{Ae^{\xi}}{(e^{\xi} - 1)^2}, \qquad\qquad (4.2)$$

where M_0 is the number of clusters, and the mass M_1 is initially given by $M_1(0) = -C_z(0, 0) = Ae^{\xi}(e^{\xi} + 1)/(e^{\xi} - 1)^3$. Solving (2.3) for the number of clusters we find

$$M_0(t) = \frac{2LM_0(0)}{(2L + aM_0(0))e^{Lt} - aM_0(0)}. \qquad\qquad (4.3)$$

The kinetic equation (2.2) can then be solved, by using the transformation $w = 1/C$ which linearises the problem and so can be solved by standard methods, which yield

$$C(z, t) = \frac{\alpha}{\beta(e^{z+\xi} - 2 + e^{-z-\xi}) - \gamma}, \qquad\qquad (4.4)$$

where

$$\alpha = \frac{4AL^2(aM_0(0) + 2L)e^{Lt}}{[aM_0(0)(e^{Lt} - 1) + 2Le^{Lt}]} \qquad\qquad (4.5)$$

$$\beta = (aM_0(0) + 2L)[aM_0(0)(e^{Lt} - 1) + 2Le^{Lt}] \qquad\qquad (4.6)$$

$$\gamma = aA(e^{Lt} - 1)(aM_0(0) + 2L). \qquad\qquad (4.7)$$

From this we obtain the explicit solution

$$c_k(t) = \begin{cases} \dfrac{\alpha}{\beta} \displaystyle\sum_{j=0}^{(k-1)/2} \binom{k-j-1}{j} (-1)^j \left(2 + \dfrac{\gamma}{\beta}\right)^{m-2j-1} e^{-k\xi}, & k \text{ odd}, \\[4mm] \dfrac{\alpha}{\beta} \displaystyle\sum_{j=0}^{(k-2)/2} \binom{k-j-1}{j} (-1)^j \left(2 + \dfrac{\gamma}{\beta}\right)^{m-2j-1} e^{-k\xi}, & k \text{ even}. \end{cases}$$

$$(4.8)$$

To assess how the width of the distribution varies in time, we calculate the standard deviation of the distribution $\sigma = \sqrt{((M_2 M_0 - M_1^2)/M_1^2)}$. This is determined by

$$\sigma^2 = \tfrac{1}{2}\text{sech}^2(\tfrac{1}{2}\xi)\left[1 + \frac{aA(e^{Lt} - 1)\cosh\xi}{aA(e^{Lt} - 1) + 8Le^{Lt}\sinh^2\tfrac{1}{2}\xi}\right]. \qquad\qquad (4.9)$$

This grows from its initial value of $\tfrac{1}{2}\text{sech}^2(\tfrac{1}{2}\xi)$ and reaches a finite width in the large-time limit. The form of the resultant distribution and its evolution in time is illustrated in Figure 6. This shows very similar to the results shown in [12, Figures 4.42, 4.43], namely, that the peak rapidly decreases in amplitude, and spreads to become a wide distribution, while its maximum hardly moves at all.

5. Conclusions

We have considered a variety of aggregation kernels which permit exact explicit solutions to be derived in the pure-aggregation case. To these coagulation equations we have added a general mass-loss term. In the case of size-independent mass-loss rates, explicit solutions are
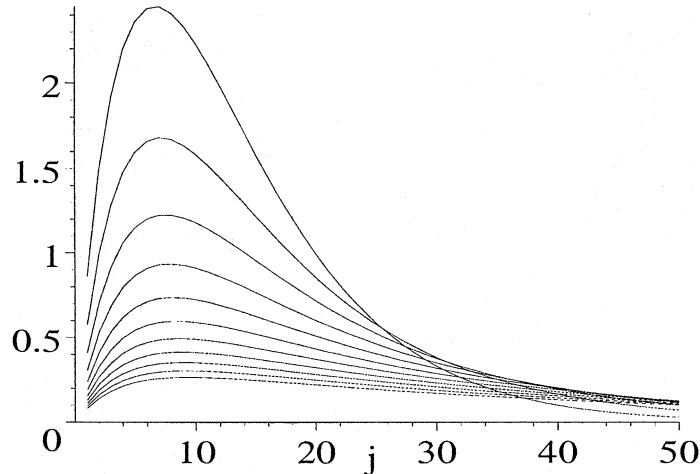
Figure 6. Plots of the distribution (4.8) in the case $L = 1$, $a = 1$, $\xi = 0{\cdot}15$, $A = 1$. The concentration $c_k(t)$ is plotted against aggregation size k for times from $t = 0$ to $t = 0{\cdot}1$ in steps of size $t = 0{\cdot}01$.

still available, and we have derived these in Section 2. Due to the presence of stirring in the system under consideration here, fractal clusters observed in Diffusion-Limited Aggregation (DLA) do not play an important role in the kinetics of growth analysed here; instead more compact aggregates are found [12].

The most interesting of these cases is the kernel $a_{i,j} = aij$, for which gelation is known to exist in the mass-conserving case. With a mass-loss term present, we find that the existence of a gelation transition depends on the strength of the mass-loss term. For small mass-loss terms, the gelation phenomenon persists, albeit with the gelation time delayed due to the presence of the mass-loss term. For stronger mass-loss terms, gelation is completely removed from the system. Our analysis precisely determines how strong the mass-loss term should be to prevent gelation.

When the mass-loss term is allowed to be size-dependent, explicit solutions are no longer available, and instead, we have sought similarity solutions. These have been found in the cases where mass-loss decreases with increasing size; in particular, in Section 3.4 we examined the case of a loss term of the form $\mathcal{L}(c_j) = Lj^\lambda c_j$ with $\lambda < 0$, for which similarity solutions have the form $c_j(t) = t^{-1+(1+2\alpha+\beta)/\lambda} f(jt^{1/\lambda})$, where the aggregation kernel is $a_{i,j} = a(ij)^\alpha(i^\beta + j^\beta)$.

The explicitly solvable case, $\lambda = 0$, shows no self-similar behaviour and so we postulate that, in the case $\lambda > 0$, similarity solutions also fail to exist. However, for $\lambda = 0$ and $a_{i,j} = a$, a solution for the cluster–distribution function has been found and fitted to an initial cluster-size distribution function containing a single hump. An explicit solution for $t > 0$ was then derived. The single-humped form of solution is seen to persist for small times, with the position of the hump staying almost static, the distribution becoming smaller in amplitude as mass is lost from the system, and much broader as aggregation creates clusters of larger sizes. This is in agreement with the numerical results of Gudmundsson for a system modelling the evolution under agglomeration of an initially single-humped distribution of TiB_2 particles in molten aluminium [12, 18].

References

1. T.A. Engh, *Principles of Metal Refining.* Oxford: Oxford University Press (1992) 564 pp..
2. C.J. Simensen, The effect of melt refining upon inclusions in aluminum. *Metall. Trans. B* 13B (1982) 31–34.
3. D.G. McCartney, Grain refining of aluminium and its alloys. *Int. Mater. Rev.* 34 (1989) 247–260.
4. J.P. Martin and F. Painchaud, On-line metal cleanliness determination in molten aluminium alloys using the LiMCA II analyser. In: *Light Metals*, V Mannweiler (ed.), Warrendale, PA: The Minerals, Metals and Materials Society (1994) pp. 915–920.
5. F. Leyvraz and H.R. Tschudi, Singularities in the kinetics of coagulation processes. *J. Phys A: Math. Gen.* 14 (1981) 3389–3405.
6. S.C. Davies, J.R. King and J.A.D. Wattis, Self-similar behaviour in the coagulation equations. *J. Eng. Math.* 36 (1999) 57–88.
7. S.C. Davies, J.R. King and J.A.D. Wattis, The Smoluchowski coagulation equations with continuous injection. *J. Phys A; Math. Gen.* 32 (1999) 7745–7763.
8. J.A.D. Wattis, S.C. Davies and J.R. King, The Smoluchowski coagulation equations with cluster-gel interactions. (2003) preprint.
9. P. Singh and G.J. Rodgers, Coagulation processes with mass-loss. *J. Phys. A. Math. Gen.* 29 (1996) 437–450.
10. E.M. Hendriks, Exact solution of coagulation equation with removal term. *J. Phys A: Math. Gen.* 17 (1984) 2299–2303.
11. H.C. Rotstein, A. Novick-Cohen and R. Tannenbaum, Gelation and cluster growth with cluster-wall interactions. *J. Stat. Phys.* 90 (1998) 119–143.
12. T. Gudmundsson, Agglomeration of TiB_2 particles in liquid aluminium. PhD thesis, Nottingham (1996) 190 pp.
13. F.P. da Costa, A finite dimensional dynamical model for gelation in coagulation processes. *J. Nonlin. Sci.* 8 (1998) 619–653.
14. M. Abramowitz and I.A. Stegun, *Handbook of Mathematical Functions.* New York: Dover (1972).
15. M. Kreer and O. Penrose, Proof of dynamic scaling in Smoluchowski's coagulation equation with constant kernels. *J. Stat. Phys.* 74 (1994) 389–407.
16. F.P. da Costa, On the dynamic scaling behaviour of solutions to the discrete Smoluchowski equations. *Proc. Edinburgh Math. Soc.* 39 (1996) 547–559.
17. E.M. Hendriks, M.H. Ernst and R.M. Ziff, Coagulation equations with gelation. *J. Stat. Phys.* 31 (1983) 519–563.
18. T. Gudmundsson, T.I. Sigfusson, D.G. McCartney, E. Wuilloud and P. Fisher, Particle collisions and inclusion removal in molten aluminium: a numerical simulation. *Mater. Sci. Forum* 217–222 (1996) 159–164.